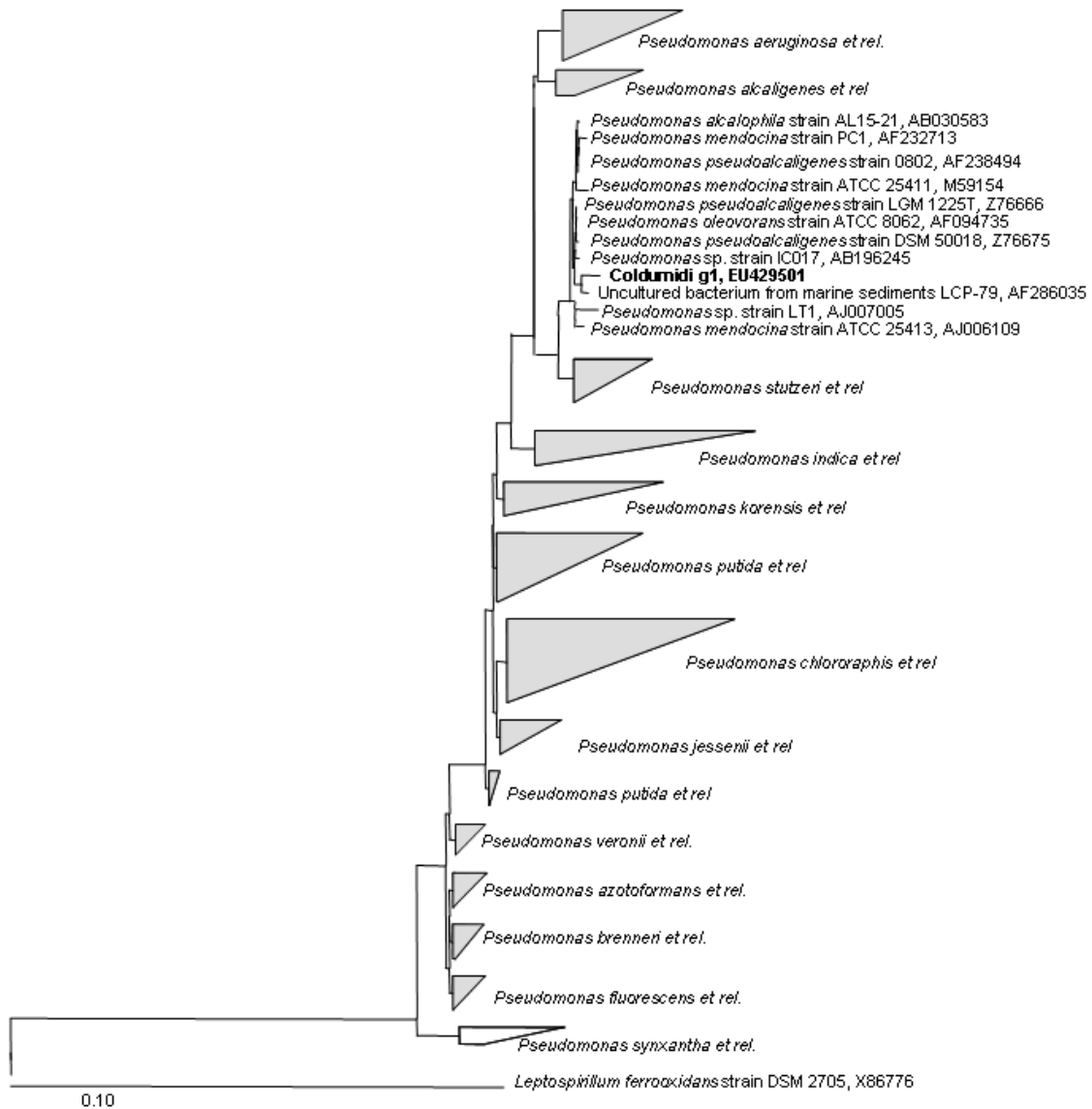
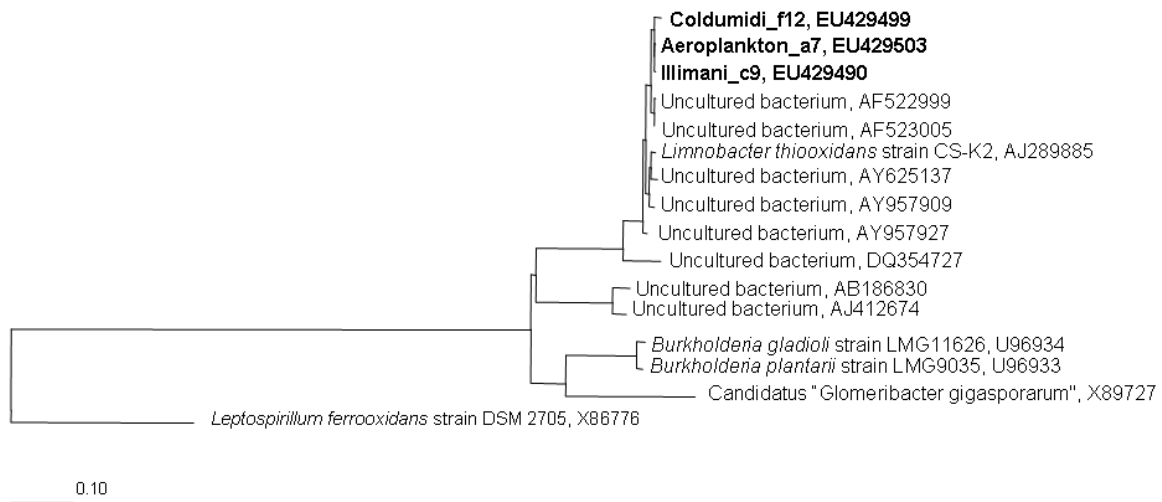


**Figure S1: Phylogenetic tree of *Pseudomonas* and related bacteria.** Phylogenetic trees were generated using parsimony, neighbor-joining and maximum likelihood analysis with different sets of filters. All generated phylogenetic trees resulted in stable branching. A consensus tree was generated using all calculated trees. Cloned 16S rRNA sequences from enrichment cultures are indicated in bold. Sequences retrieved from Col du Midi (Alps) are designated by the word “Coldumidi” followed by the number of the sequence. Bar represents 10% estimated phylogenetic divergence.



**Figure S2: Phylogenetic tree of *Limnobacter* and related bacteria.** Phylogenetic trees were generated using parsimony, neighbor-joining and maximum likelihood analysis with different sets of filters. All generated phylogenetic trees resulted in stable branching. A consensus tree was generated using all calculated trees. Cloned 16S rRNA sequences from enrichment cultures are indicated in bold. Sequences retrieved from Nevado Illimani (Andes) are designated by the word “Illimani” followed by the number of the sequence. Sequences from Col du Midi (Alps) are designated by “Coldumidi” followed by the number of the sequence. Sequences from aerosol sample recollected in Antarctica are designated by “Aeroplankton” followed by the number of the sequence. Bar represents 10% estimated phylogenetic divergence.



**Figure S3: Phylogenetic tree of *Dietzia* and related bacteria.** Phylogenetic trees were generated using parsimony, neighbor-joining and maximum likelihood analysis with different sets of filters. All generated phylogenetic trees resulted in stable branching. A consensus tree was generated using all calculated trees. Cloned 16S rRNA sequences from enrichment cultures are indicated in bold. Sequences retrieved from Col du Dome (Vallot, Alps) are designated by “Vallot” followed by the number of the sequence. Bar represents 10% estimated phylogenetic divergence.

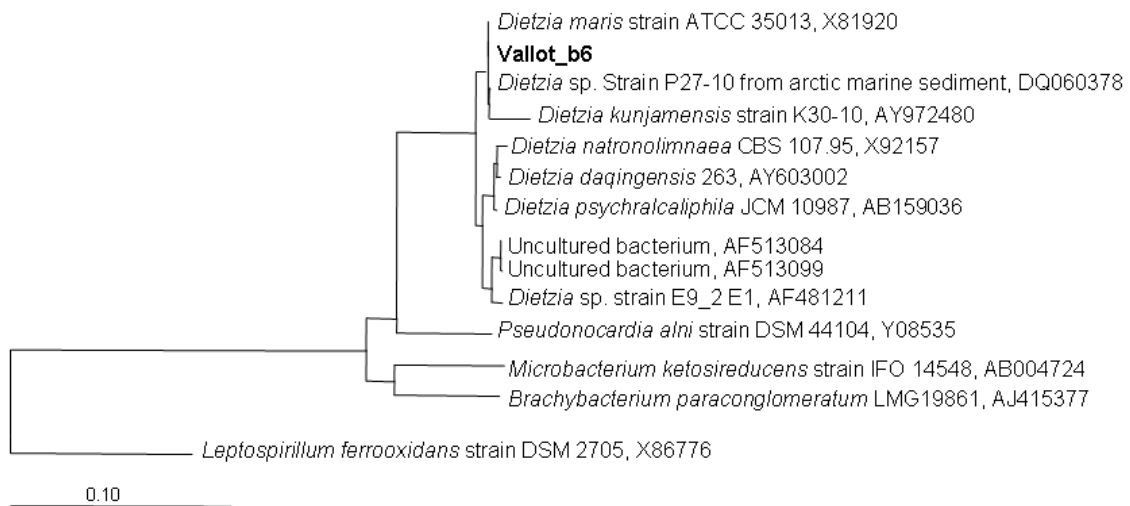


**Figure S4: Phylogenetic tree of *Brachybacterium* and related bacteria.** Phylogenetic trees were generated using parsimony, neighbor-joining and maximum likelihood analysis with different sets of filters. All generated phylogenetic trees resulted in stable branching. A consensus tree was generated using all calculated trees. Cloned 16S rRNA sequences from enrichment cultures are indicated in bold. Sequences retrieved from aerosol sample recollected in Antarctica are designated by “Aeroplankton” followed by the number of the sequence. Bar represents 10% estimated phylogenetic divergence.

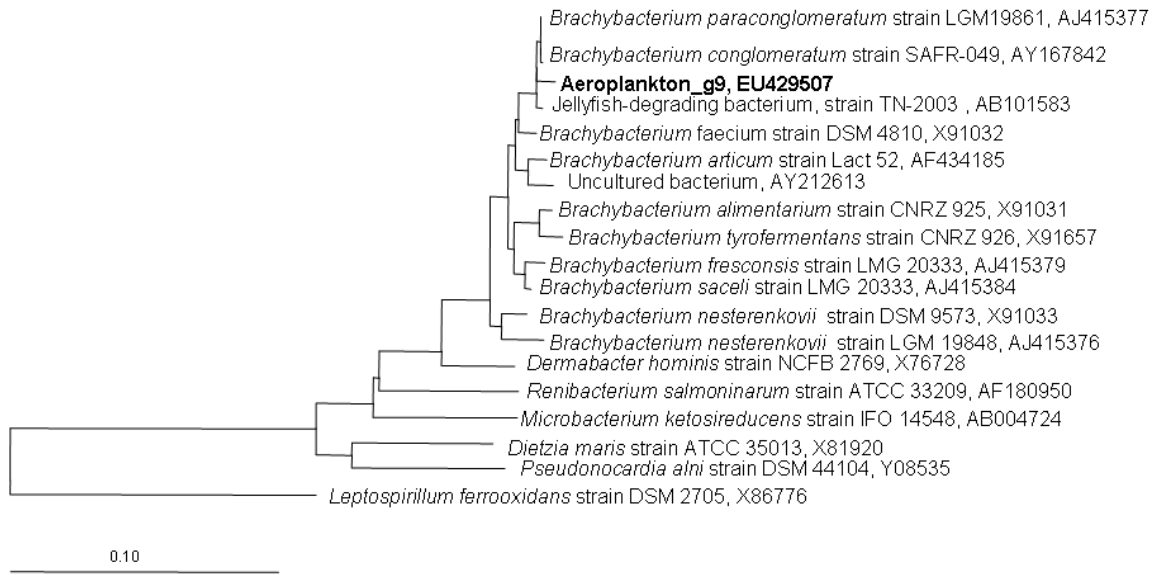


**Figure S5: Phylogenetic tree of *Microbacterium* and related bacteria.** Phylogenetic trees were generated using parsimony, neighbor-joining and maximum likelihood analysis with different sets of filters. All generated phylogenetic trees resulted in stable branching. A consensus tree was generated using all calculated trees. Cloned 16S rRNA sequences from enrichment cultures are indicated in bold. Sequences retrieved from Nevado Illimani (Andes) are designated by the word “Illimani” followed by the number of the sequence. Bar represents 10% estimated phylogenetic divergence.

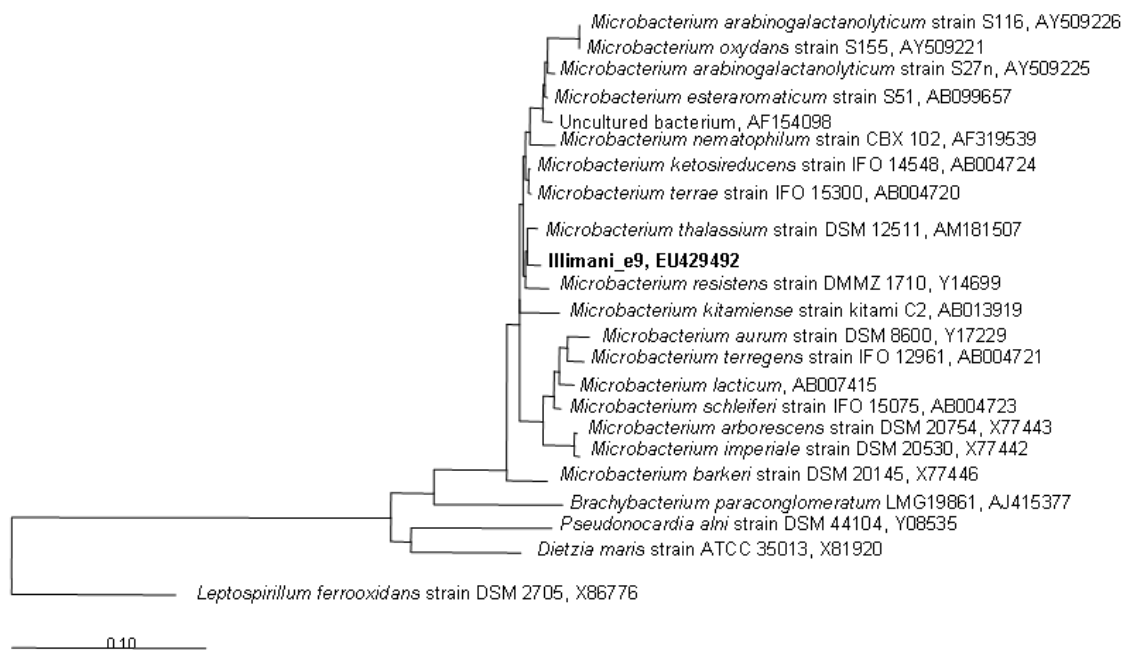


**Figure S6: Phylogenetic tree of *Afipia* and related bacteria.** Phylogenetic trees were generated using parsimony, neighbor-joining and maximum likelihood analysis with different sets of filters. All generated phylogenetic trees resulted in stable branching. A consensus tree was generated using all calculated trees. Cloned 16S rRNA sequences from enrichment cultures are indicated in bold. Sequences retrieved from Nevado Illimani (Andes) are designated by the word “Illimani” followed by the number of the sequence. Sequences from Col du Midi (Alps) are designated by “Coldumidi” followed by the number of the sequence. Sequences from aerosol sample recollected in Antarctica are designated by “Aeroplankton” followed by the number of the sequence. Sequences retrieved from Col du Dome (Vallot, Alps) are designated by “Vallot” followed by the number of the sequence. Bar represents 10% estimated phylogenetic divergence.

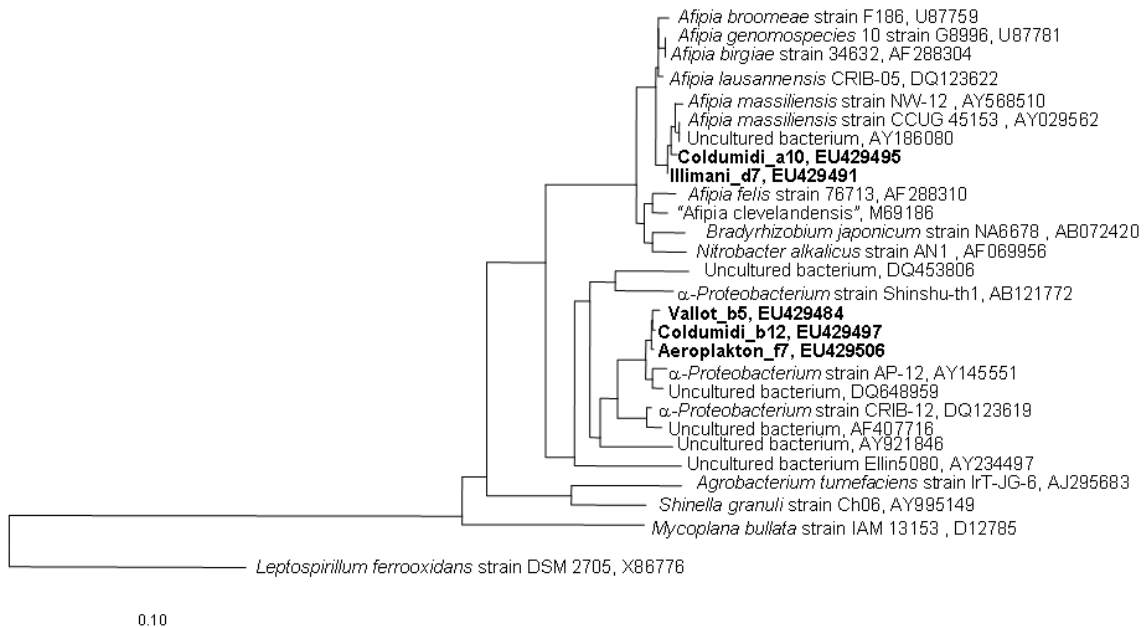


**Figure S7: Phylogenetic tree of *Shinella* and related bacteria.** Phylogenetic trees were generated using parsimony, neighbor-joining and maximum likelihood analysis with different sets of filters. All generated phylogenetic trees resulted in stable branching. A consensus tree was generated using all calculated trees. Cloned 16S rRNA sequences from enrichment cultures are indicated in bold. Sequences retrieved from Col du Dome (Vallot, Alps) are designated by “Vallot” followed by the number of the sequence. Bar represents 10% estimated phylogenetic divergence.

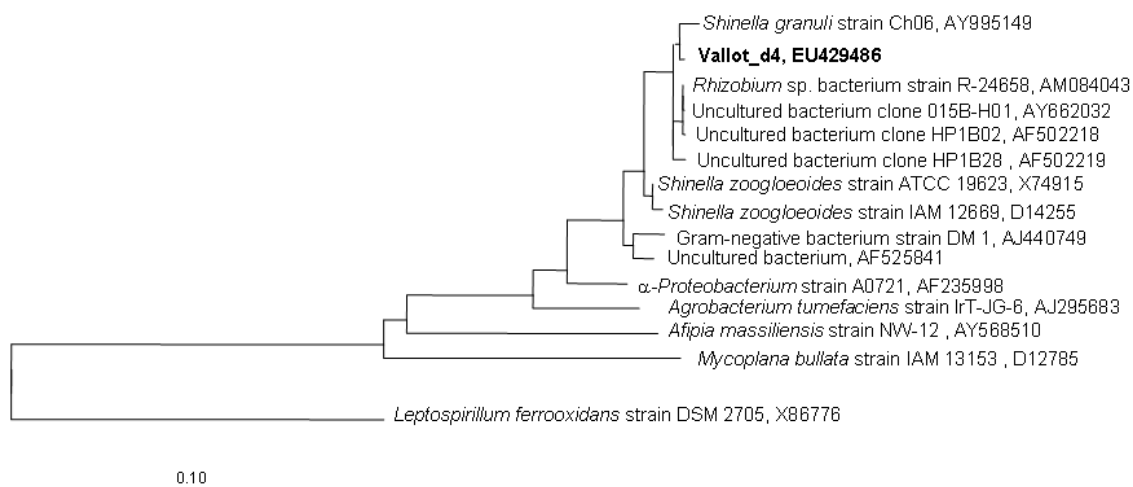


**Figure S8: Phylogenetic tree of *Brevundimonas* and related bacteria.** Phylogenetic trees were generated using parsimony, neighbor-joining and maximum likelihood analysis with different sets of filters. All generated phylogenetic trees resulted in stable branching. A consensus tree was generated using all calculated trees. Cloned 16S rRNA sequences from enrichment cultures are indicated in bold. Sequences retrieved from Nevado Illimani (Andes) are designated by the word “Illimani” followed by the number of the sequence. Sequences from aerosol sample recollected in Antarctica are designated by “Aeroplakton” followed by the number of the sequence. Sequences from Uruguay Antarctic Station Artigas are designated by “Artgas” followed by the number of the sequence. Bar represents 10% estimated phylogenetic divergence.

